Ligand-based design, in silico ADME-Tox filtering, synthesis and biological evaluation to discover new soluble 1,4-DHP-based CFTR activators

Ligand-based design, *in silico* ADME-Tox filtering, synthesis and biological evaluation to discover new soluble 1,4-DHP-based CFTR activators

*Sonia Visentin[$], Giuseppe Ermondi[$], Claudio Medana§, Nicoletta Pedemonte†, Luis Galietta† and Giulia Caron[$]**

[$] CASSMedChem Research Group, DSTF at the Centre for Innovation, Università di Torino, Via Quarello 11, 10135 Torino, Italy.

[§] Dipartimento di Chimica Analitica, Università di Torino, via Giuria 5, 10125 Torino, Italy.

[†] Laboratorio di Genetica Molecolare, Istituto Giovannina Gaslini, Largo Gerolamo Gaslini 5, 16147 Genova, Italy

E-mail: giulia.caron@unito.it

Abbreviations: CF, Cystic fibrosis; CFTR, Cystic fibrosis transmembrane conductance regulator; ADME-Tox, Absorption Distribution Metabolism Toxicity; DHP, 1,4-dihydropyridine; QSAR, Quantitative Structure-Activity Relationships; L-VDCC, L-type voltage-dependent Ca^{2+} channels; MIFs, Molecular Interaction Fields; GRIND, GRID Independent Descriptors, PLS, Partial Least Squares.

ABSTRACT

The altered gating of the mutant CFTR chloride channel cystic fibrosis (CF) may be corrected by small molecules called potentiators. We present a molecular scale simulation system for the discovery of ΔF508-CFTR soluble potentiators. Results report the design, ADME-Tox prediction, synthesis, solubility determination and in vitro biological evaluation of two 1,4-dihydropyridines (DHPs). Compound **1** shows a promising ADME-Tox profile and good potency.

KEYWORDS: DHP, 3D-QSAR, ADME-Tox, CFTR potentiators, GRIND, VolSurf+.

Introduction

Cystic fibrosis (CF), a serious disease afflicting about 1 in 2500 individuals in the Caucasian population, is caused by inherited mutations in the CF transmembrane conductance regulator (CFTR) gene [1]. The product of this gene is a plasma membrane protein with Cl^-channel function [2]. The most common disease-causing mutation of CFTR is ΔF508, a deletion of phenylalanine at position 508 [3]. ΔF508 impairs the maturation of as well the gating of CFTR protein. Instead, other mutations such as G551D and G1349D cause only a gating defect.

Small-molecule therapy for CF-causing mutations is thought to have considerable promise [4] but to the best of our knowledge only one structure-based virtual screening strategy [5] and no ligand-based approach for the discovery of new CFTR modulators is reported in the literature (some QSAR and SAR studies were performed *a posteriori* after synthesis and biological testing of compounds [6-9]). Ligand-based design methods capitalize on the fact that ligands similar to an active ligand are more likely to be active than random ligands. This approach could be extremely useful for CFTR potentiators because the lack of a high resolution 3D structure of the full length protein prevents a clear strategy for designing compounds that act by direct interaction with CFTR to be defined [5]).

1,4-dihydropyridines (DHPs) used to treat hypertension also act as CFTR potentiators, i.e. pharmacological compounds restoring the activity of CFTR mutants with defective gating [10]. As antihypertensive agents, DHPs act by blocking L-type voltage-dependent Ca^{2+} channels (L-VDCC) and therefore cause the relaxation of arterial smooth muscle cells [11]. It was also found that mutant CFTR is activated by DHPs through a mechanism not involving the modulation of Ca^{2+} channels, but by a probable direct interaction with the CFTR protein itself [11].

DHP is considered a privileged scaffold by medicinal chemists since a large amount of information is available on pharmacokinetics and toxicity properties and its chemical accessibility could enable, in case of success, a rapid start of clinical trials [12]. However, the ability of DHPs to interact with a number of pharmacological targets is also the source of selectivity issues [12].

Pedemonte et al. in 2007 [6] identified four DHPs of potential interest (DHP106, DHP194, DHP229 and DHP256, Figure 1) since endowed with a potency as CFTR potentiators higher than that as Ca^{2+} channel blockers, the opposite of what is found for anti-hypertensive DHPs such as felodipine.

However, the novel DHPs are expected to be poorly soluble in water (see below).

Figure 1

This study firstly describes a molecular scale simulation system to check the feasibility of discovering new soluble CFTR potentiators based on the DHP scaffold. Then the two molecules of potential interest resulting from the in silico studies were synthesized, submitted to aqueous solubility measurements and tested as CFTR activators with a functional assay (methods for evaluating direct binding to the full length CFTR or its ΔF508 mutant are currently unavailable) based on the measurement of CFTR-mediated anion transport.

Results and discussion

The whole design procedure consisted in five steps: a) building and interpretation of a robust 3D-QSAR model for a series of 105 DHPs active as CFTR potentiators; b) set-up of a 3D-QSAR model able to predict Ca^{2+} channel blockade; c) in silico solubility analysis; d) design of new structures on the basis of the information arising from the previous steps and e) check of the two candidates for their ADME-Tox and solubility profiles.

3D-QSAR model of DHPs as CFTR activators

From the dataset of felodipine analogues discussed by Pedemonte et al. [6], the molecules with numerical (we selected to include in the dataset only the molecules that have numerical measured values of biological activity and we decided not to include the molecules that have only "text " values, e.g - "higher than") K_d values as CFTR activators were selected (105) and then split in a training (66) and a test set (37).

Among the plethora of descriptors today available to build 3D-QSAR models, we decided to use Molecular Interaction Fields [13, 14] based descriptors, i.e. the GRID Independent Descriptors

(GRIND) [15, 16] because they were successfully used in many cases to model pharmacodynamics activities [17, 18]. After building the 3D structures, GRIND descriptors were calculated both for the training and the test set using Pentacle as software (see Experimental Part).

According to the OECD principles of QSAR validation [19] as an essential requirement for QSAR studies, the GRIND-based 3D-QSAR model was built. To do that, the K_d values (dF508-CFTR, μM) were transformed in pK_d (the larger the more potent) and related to GRIND descriptors by a PLS algorithm. Statistical results are in Table 1 and prove that a robust model was found.

Table 1

The test set prediction was convincing: SDEP is 0.34 and values close to 1 for the slope and close to 0 for the Y-intercept in the linear regression relating experimental and calculated values were calculated (Figure 2). For three compounds (DHP008, DHP054 and DHP183) the difference between experimental and calculated values is larger than one logarithmic unit. This discrepancy could not be attributed to the presence of a nitro group in *meta* and *para* position on the DHP aromatic ring (present both in DHP008 and DHP054) since this feature is also present in structures whose pK_d is well predicted. The bad prediction of DHP183 could be due to the peculiar aromatic substitutions.

Figure 2

The CFTR activator model was submitted to chemical interpretation as discussed below. Figure 3 shows the most relevant GRIND for three compounds: two good CFTR potentiators, DHP194 and DHP242, and one with poor biological activity, DHP138 (distances in red are favorable, i.e distances that increase biological activity, whereas distances in blue are not favorable i.e distances that decrease biological activity). Of particular relevance in DHP194 the unfavorable (blue) distance between red (due to the O probe) and green (due to the TIP probe) crosses (d1 in Figure 3) that indicates that the regions defining the corresponding spatial extents probably do not fit well into the receptor binding pockets, i.e. steric hindrance. A second unfavorable (blue) distance related to steric limits is d2 in Figure 3. This distance suggests that to obtain good CFTR potentiators it is preferable to avoid large substituents in 2

and 6.

Figure 3

3D-QSAR model of DHPs as calcium channel blockers

Here binary values (see Experimental Part) were related to the GRIND descriptors by a PLS algorithm. Results are in Table 1 and show that also for the Ca^{2+} channel blocking activity a good statistical model was found. The five compounds badly predicted (three false positives and two false negatives, see Experimental Part) were close to the threshold value selected to distinguish very active from less active compounds.

Once statistically validated, we verified that the model caught most of the structural features important for Ca^{2+}-channel-blocking activity reported in the literature [12]. As an example, an unsubstituted NH group (R1 = H) in the DHP ring is important for the blocking action. This is shown in Fig. 4 for DHP 147 (binary value = -1) for which a number of unfavorable distances (blue) are located close to the methylated DHP nitrogen. The rules for Ca^{2+}-channel-blocking activity associated to the substitution at the phenyl ring at R4 are also verified by our model. The requirements of a substituent at the phenyl group for optimal activity include: a) a bulky substituent at the ortho position; b) a bulky but not lengthy substituent at the meta-position and c) a small substituent at the para-position. This is shown in Fig. 3 for DHP184 (binary value = -1) that exhibits a large substituent in para position connected by an unfavourable (blue) distance to the hydrophobic region of the DHP. The ester substituents at R3 and R5 and substituents at R2 and R6 that greatly influence the potency and selectivity of the DHP's are also retrieved by the model (data not shown).

Figure 4

Solubility analysis

The aqueous solubility at pH = 7.5 was calculated using the model implemented in VolSurf+ [20]. Results (Figure 5) evidenced that most of the active compounds of the original dataset (also the four most promising in Figure 1) could present solubility problems *in vivo* since they are largely less soluble

than nifedipine (-3.72).

Figure 5

Design

The main aim of the design step was to maximize potency, selectivity and aqueous solubility of molecules bearing the DHP scaffold. To do that we firstly focused on obtaining structures active as CFTR potentiators. According to Fig. 3 guidelines, we firstly selected a DHP scaffold bearing methyl groups in position 3 and 5 and a phenyl ring *meta* substituted with a nitro group in position 4.

To improve solubility we decided to introduce a polar moiety and in particular a nitrooxyl group since a) some DHPs bearing a nitrate are already described in the literature (see above) [21, 22] b) among polar groups OHs are detrimental for CFTR potency [6] and c) a basic amino group was discarded because it could be related to diffusion-limited rate issues [23].

The calcium channel blocking activity was not specifically minimized but any proposed structure with expected good CFTR potency and solubility was checked for its Ca^{2+} channel antagonism by the aid of the QSAR model described above.

Compound **1** in Figure 6 was finally proposed as a compound with a promising medicinal chemistry profile (calculated pK_d : 5.89) whereas **2** (calculated pK_d : 5.47) was individuated as a compound of interest to validate the molecular scale simulation system.

Figure 6

Compounds **1** and **2** were then submitted to calculations to obtain ADME-Tox and physicochemical descriptors (Table S3). In particular the molecules were projected on the following pre-calculated models implemented in VolSurf+ [20]: aqueous solubility at pH = 7.5 and log P, Caco-2 cell permeability, plasma protein affinity, blood–brain barrier permeation and metabolic stability. The models are based on VolSurf+ descriptors that in turn are obtained from MIFs by calculating the volume or the surface of the interaction contours at predefined energy values [20].

The ADME-Tox profiles of drug-likeness **1** and **2** were evaluated according to the rules proposed by

Carosati et al. [24]. Nifedipine data were calculated and reported as a comparison. The physico-chemical and pharmacokinetic descriptors (Table 2) were fully convincing since all values are in line with alert threshold values [24]. According to solubility predictions, **1** shows a better profile than molecules present in the original dataset whereas **2** could be ranked in an intermediate position (Figure 5).

Finally, hERG toxicity was predicted on the basis of a QSAR model recently published by some of us [25] by using the threshold value of 6 (pIC_{50} units) to distinguish active (i.e. potentially toxic) from not active compounds [26]. Results indicate that some concerns could arise for **2** since the predicted hERG toxicity value is larger (6.20) than suggested threshold value (6.0, see above).

Table 2

Chemistry

The procedure to obtain **1** is described in the literature [21] The racemic compound (±) **2** was prepared by synthetic route as depicted in Scheme 1, which involved use of a modification of Hantzsch reaction. 3-Nitrooxypropyl-3-amino-2-butenoate **c** [23] was condensed with 3-nitrobenzaldehyde **a** and nitroacetone **b** to afford a racemic mixture of **2**.

Scheme 1

Physicochemical and biological evaluation

Experimental solubility of nifedipine, **1** and **2** was then determined at pH 7.4 in phosphate buffer and the following data in –lgS 7.5 (mg/L) were found: **1** -4.88 (5.3 ± 0.3), **2** -4.88 (5.8 ± 1.2), and nifedipine -4.18 (22.6 ± 12.2). Compounds **1** and **2** are thus slightly less soluble than nifedipine but more soluble than most compounds of the investigated dataset. These data also show some limits in the VolSurf+ predictions.

Bearing a nitrooxyl group, the final DHPs **1** and **2** were assessed for their ability to generate NO in the presence of a large excess of cysteine (1:50) in buffer solution (pH 7.4) at 37 °C. The extent of NO production after 1 h was determined by detection of nitrite, which is the oxidative metabolite of nitric

oxide (Griess reaction). Results show that in these experimental conditions neither **1** nor **2** are able to release nitric oxide (< 0.5 % NO_2^-).

We then determined dose–response relationships for **1** and **2** as ΔF508-CFTR potentiators. For this purpose, we utilized the functional assay based on the halide-sensitive yellow fluorescent protein, HS-YFP [11]. Cells are first incubated at low temperature to rescue the mutant protein from the endoplasmic reticulum allowing its targeting to the plasma membrane. Then cells are acutely stimulated with a high concentration of the adenylyl cyclase inhibitor forskolin, to allow maximal ΔF508-CFTR phosphorylation, in the absence or presence of test compounds. ΔF508-CFTR activity is measured as the rate in HS-YFP fluorescence quenching caused by iodide influx, as previously described [11]. True potentiators increase activity above the level obtained with forskolin alone. This was the case for compounds **1** and **2**. Fitting of data obtained at different concentrations with a Hill equation allowed to estimate apparent K_d and maximal effect. The following K_d values were determined: 1.3 μM for **1** and 3.4 μM for **2** (corresponding pK_d values, 5.88 and 5.07, respectively), in good agreement with calculated values (5.89 and 5.47). Maximal effect of these compounds was comparable to that of the most effective DHPs previously tested [11].

Summing-up the new strategy here proposed enabled to discover **1** as a CFTR potentiator of potential interest and to highlight the limits of **2**. Moreover, results also showed that the insertion of a nitrooxyl group on the 1-4-DHP supports CFTR potency.

Conclusions

Effective CFTR potentiators are very useful for the treatment of CF patients affected by mutations that cause impaired CFTR channel gating. Among the various families of chemical compounds showing potentiator activity, DHPs are particularly interesting because of existing information on medicinal chemistry and pharmacological properties.

Our study presents a new ligand-based strategy to discover novel DHPs potentiators with improved drug-like characteristics. In particular here for the first time a 3D-QSAR model able to predict the

CFTR activation properties is described and experimentally validated. Since this model is combined with computational strategies to predict calcium channel blocking activity and ADME-Tox filtering procedures, the study as a whole sounds very promising in the development of strategies to discover drug candidates for CF therapy.

Nevertheless the solid design procedure is necessary but not sufficient to discover highly potent, selective and soluble CFTR potentiators based on the DHP scaffold since solubility seems to negatively affect CFTR potentiators potency. This could be related to some hydrophobic features of the receptor responsible for CFTR activity. This point could be clarified on the basis of a high-resolution 3D structure of CFTR in complex with one validated activator currently unavailable.

Experimental Part

Molecular modeling

To build the 105 structures two automatic builders (Frog 2.1 (http://bioserv.rpbs.univ-paris-diderot.fr/cgi-bin/Frog2) and MOE) were used and two datasets (called Frog_ds and MOE_ds, respectively) were prepared. Since only a modest stereoselectivity was observed in previous studies for niguldipine, BayK-8644 and isradipine [11], the stereochemistry proposed by the automatic tools was maintained (R for MOE and S for Frog). Frog_ds and MOE_ds were submitted to AM1 minimization which yelded Frog_ds_min and MOE_ds_min, respectively. Four datasets were thus built to check the dependence of the models on the adopted 3D building strategy. This approach was chosen both on the basis of a previous work [27] and also to take into account the controversial reports in the literature about DHPs structural features: DHP of the nifedipine type are flexible molecules, in which the C-4-aryl moiety and the C-3 and C-5 ester substituents can rotate and the conformation of the DHP ring can change [12]. Preliminary tests (data not reported) showed that the best models are found by using the 3D structures arising from Frog builder and minimized with AM1 semi empirical method. All remaining models based on different training sets were of slightly lower quality and their chemical interpretation did not significantly differ from the one reported below.

The final structures were saved in mol2 format, randomly split in training (66) and test sets (39) and submitted to Pentacle (version 1.0.5, Molecular Discovery Ltd. Pinner, Middlesex, UK, 2010, http://www.moldiscovery.com), and VolSurf+ (version 1.0.4, Molecular Discovery Ltd. Pinner, Middlesex, UK, 2009, http://www.moldiscovery.com).

A standard procedure to build 3D-QSAR models already described by some of us [27] was used in Pentacle. Briefly, four probes (DRY, O, N1 and TIP) and default values for all Pentacle parameters were used; MIFs filtering and encoding tools were combined to produce four sets of GRIND descriptors: ALMOND/MACC2, ALMOND/CLACC, AMANDA/MACC2 and AMANDA/CLACC. We built models with the four sets and selected the model with the best statistical performance (AMANDA/CLACC for both models). Since the L-VDCC inhibition percentage at 1 μM reported in the original paper [6] is not an appropriate biological endpoint because of the nonlinear characteristic of dose/response relationships, for the calcium channel blocking model we decided to adopt a simple binary classification of data [18]. Compounds with the L-VDCC inhibition percentage larger than 80% were set as active (value=1) whereas compounds with this percentage smaller or equal to 80% were set inactive (value=-1). This classification is arbitrary but it takes into account the high-throughput format of the data and their distribution (see Supporting Information). In our opinion it is acceptable to build a fast screening model to use as a support in a more complex design program.

The 3D structures were submitted to VolSurf+ using default settings and four probes (OH2, DRY N1 and O probes that mimic respectively water, hydrophobic, hydrogen bond acceptor and hydrogen bond donor interaction of the compounds with the environment) [18, 20]. The molecules were projected on the pre-calculated models implemented in VolSurf+ to calculate ADME-Tox parameters and solubility.

PCA and PLS tools implemented in Pentacle were used. In addition XLStat v.2009.6.04 (www.xlstat.com) was also used to obtain the VIP plots.

All calculations were performed on a Linux based server and on standard PCs operating with Microsoft Windows 7.

Chemistry

Melting points were determined on a Büchi 530 apparatus after introducing the sample into the bath at a temperature 10 °C lower than the melting point. A heating rate of 1 °C min^{-1} was used, 3 °C min^{-1} in the case of decomposition. The compounds were routinely checked by infrared spectrophotometry (Shimadzu FT-IR 8101). ^{1}H and ^{13}C NMR spectra were recorded on a Bruker AC-200 spectrometer and are reported in ppm units (* means either not assigned or tentatively assigned). All of the spectra were in keeping with the structures. Column chromatography was performed on silica gel (Merck Kieselgel 60, 230-400 mesh ASTM) with the indicated solvent system. Anhydrous $MgSO_4$ was used as a drying agent. Solvent removal was achieved under reduced pressure at room temperature. Elemental analyses of the new compound was performed by REDOX (Cologno Monzese), and the result is within 0.4% of the theoretical values.

Synthesis of (±)3-Nitrooxypropyl 1,4-Dihydro-2,6-dimethyl-5-nitro-4-(3-nitrophenyl)pyridine-3-carboxylate (compound **2**)**:** A mixture of 3-nitrobenzaldehyde (0.73 g, 5 mmol) and nitroacetone (1.8 g, 17.5 mmol) in 2-propanol (40 mL) was refluxed for 4h. 3-Nitrooxypropyl-3-amino-2-butenoate (1.08 g, 5 mmol) was added and heating was continued for other 4 h; solvent removal gave a residue which was purified by flash-chromatography (petroleum ether 6 / ethyl acetate 4). The yellow solid was recrystallized from $CHCl_3$/PE. Yield 30%; mp154°C.

^{1}H-NMR (DMSO-d_6): 1.967 (q, 2H, CCH_2C); 2.34 (s, 3H, 6-CH_3); 2.52 (s, 3H, 2-CH_3); 4.08 (t, 2H, CH_2ONO_2); 4.42 (t, 2H, OCH_2); 5.36 (s, 1H, 4-CH); 7.54-8.07 (m, 4H, Ph); 9.79 (s br, 1H, NH).

^{13}C-NMR (DMSO-d_6): 17.95 (2-CH_3); 19.67 (6-CH_3); 25.68 (CCH_2C); 39.60 (C4-DHP); 60.56 (OCH_2); 70.85 (CH_2ONO_2); 105. 24 (C5-DHP); 125.75 (C3-DHP); 121.92 , 122.25, 129.90, 134.53, 145.31*, 147.09*(Ph); 147.85*, 148.17* (C2,C6-DHP); 165.82 (COO) (*tentatively assigned).

Cell culture

Fischer rat thyroid (FRT) cells with stable co-expression of ΔF508-CFTR and the halide-sensitive yellow fluorescent protein YFP-H148Q/I152L [11] were cultured at 37 °C (5% CO_2 atmosphere) in

Coon's modified Ham's F-12 medium plus 10% fetal calf serum, 2 mM L-glutamine, 100 U/ml penicillin, and 100 μg/ml streptomycin. Zeocin (0.6 mg/ml) and G418 (0.75 mg/ml) were also included in the medium to maintain selection for mutant CFTR and the fluorescent protein expression, respectively. For the functional assay performed with a microplate reader, cells were plated in black-wall clear-bottom 96-well microplates (Corning 3603) at a density of 50,000 cells per well. After 24 hours from plating, cells were incubated for further 20-24 hours at 27 °C to rescue ΔF508-CFTR to the cell surface [11].

Fluorescence assay for CFTR activity

Cells were washed with PBS (containing 137 mM NaCl, 2.7 mM KCl, 8.1 mM Na_2HPO_4, 1.5 mM KH_2PO_4, 1 mM $CaCl_2$ and 0.5 mM $MgCl_2$) and stimulated for 30 min with forskolin (20 μM) with or without test compounds at different concentrations. The cells were then transferred to a microplate reader (FluoStar Galaxy; BMG Labtech GmbH, Offenburg, Germany) for CFTR activity determination. The plate reader was equipped with high-quality excitation (ET500/20X: 500 ± 10 nm) and emission (ET535/30M: 535 ± 15 nm) filters for YFP (Chroma Technology Corp., Brattleboro, VT). Each assay consisted of a continuous 14-s fluorescence reading with 2 s before and 12 s after injection of an iodide-containing solution (PBS with Cl^- replaced by I^-; final I^- concentration in the well: 100 mM). Data were normalized to the initial background-subtracted fluorescence. To determine fluorescence quenching rate (QR) associated with I^- influx, the final 11 s of the data for each well were fitted with an exponential function to extrapolate initial slope (dF/dt).

Solubility

The solubility was evaluated introducing an excess of analyte (nifedipine, compounds **1**, **2**) in a volumetric flask in concentrated (10 mg/mL) methanolic solution and allowing it to evaporate before the addition of the solvent buffer (50 mM phosphate buffer, pH 7.4).

The concentration of the supernatant solution was determined after 30 minutes of solubilization treatment in a ultrasound bath at room temperature by HPLC-UV-MS using a Dionex Ultimate 3000

chromatographic system, (Dionex, Milan, Italy) equipped with two detectors: Surveyor DAD detector and LTQ-Orbitrap (Thermo Scientific, Rodano, Italy) spectrometer, with electrospray interface and ion trap as high resolving power mass analyzer. The chromatographic separations were run on a Phenomenex Luna C18 column (150 × 2 mm, 3 μm particle size) (Phenomenex, Torrance, CA, USA). Flow rate was 200 μL min^{-1}. Gradient mobile phase composition was adopted: 70/30 to 100/0 v/v 0.05% formic acid in water/methanol in 30 min. Quantitation was done integrating the UV signal (240 nm) chromatogram and the identity of the compounds was confirmed by mass spectrometry. Mass spectra were collected in tandem MS mode for the following ions 347 (nifedipine), 423 (**2**) or 436 (**1**) *m/z*. The retention times of the investigated compounds were 21.0 (nifedipine), 23.2 (**2**) or 24.4 (**1**) minutes.

NO release

Nitrite production by $–ONO_2$ in the presence of L-cysteine was evaluated according to the procedure described in the details elsewhere [28]**.** A solution of compounds **1** and **2** (20 μL) in DMSO was added to 2 mL of 50 mM phosphate buffer (pH 7.4), containing 5 mM L-cysteine. The final concentration of drug was 10^{-4} M. After 1 h at 37°C, 1 mL of the reaction mixture was treated with 250 μL of the Griess reagent (4 g sulfanilamide; 0.2 g N-naphtylethyldiamine dihydrochloride; 10 mL 85% phosphoric acid in distilled water. After 10 min at room temperature, absorbance was measured at 540 nm (Perkin-Elmer Lambda 5 spectophotometer). 10-880 nmol/mL sodium nitrite standard solution were used for the calibration curve. The yield in nitrite was expressed as NO_2^- % (mol/mol).

Supporting Information Available: Experimental and calculated CFTR activation data (pK_d) and filtered MIFs for **1** and **2,** calcium channel blocking 3D-QSAR model details, the whole set of VolSurf+ descriptors.

REFERENCES

[1] Bush, A. Cystic Fibrosis in the 21st Century. (Bush A, ed.) 2006.

[2] J.R. Riordan, CFTR function and prospects for therapy. Annu. Rev. Biochem. 77 (2008) 701-26.

[3] A.S. Verkman, L.J.V. Galietta, Chloride channels as drug targets. Nat. Rev. Drug Discov. 8 (2009) 153-171.

[4] N. Pedemonte, G.L. Lukacs, K. Du, E. Caci, O. Zegarra-Moran, L.J.V. Galietta, A.S. Verkman, Small-molecule correctors of defective Δ F508-CFTR cellular processing identified by high-throughput screening. J.Clin.Invest. 115(9) (2005) 2164-2571.

[5] O. Kalid, M. Mense, S. Fischman, A. Shitrit; H. Bihler, Small molecule correctors of F508del-CFTR discovered by structure-based virtual screening. Comput. Aid. Mol. Des. 24 (2010) 971-991.

[6] N. Pedemonte, D. Boido, O. Moran, M. Giampieri, M. Mazzei, R. Ravazzolo, G. Galietta, Structure-Activity Relationship of 1,4-Dihydropyridines as Potentiators of the Cystic Fibrosis Transmembrane Conductance Regulator Chloride Channel. Mol. Pharmacol. 72 (2007) 197-207.

[7] F. Cateni, M. Zacchigna, N. Pedemonte, G. Galietta, M.T. Mazzei, P. Fossa, M. Giampieri, M. Mazzei, Synthesis of 4-thiophen-2 0 -yl-1 , 4-dihydropyridines as potentiators of the CFTR chloride channel. Bioorg. Med. Chem. 17(23) (2009) 7894-7903.

[8] M. Springsteel, Benzoflavone activators of the cystic fibrosis transmembrane conductance regulator: towards a pharmacophore model for the nucleotide-binding domain. Bioorg. Med. Chem. 11(18) (2003) 4113-4120.

[9] H. Yang, A.A. Shelat, R.K. Guy, V.S. Gopinath, T. Ma, K. Du, G.L. Lukacs, A. Taddei, C. Folli, N. Pedemonte, L.J.V. Galietta, A.S. Verkman, Nanomolar Affinity Small Molecule Correctors of Defective ΔF508-CFTR Chloride Channel Gating. J. Biol. Chem. 278(37) (2003) 35079 -35085.

[10] R. Budriesi, P. Ioan, A. Leoni, N. Pedemonte, A. Locatelli, M. Micucci, A. Chiarini, L.J.V. Galietta, Cystic Fibrosis: A New Target for 4-Imidazo[2,1-b]thiazole-1,4-dihydropyridines. J.Med.Chem. 54 (2011) 3885–3894.

[11] N. Pedemonte, T. Diena, E. Caci, E. Nieddu, M. Mazzei, R. Ravazzolo, O. Zegarra-Moran,

L.J.V. Galietta, Antihypertensive 1,4-Dihydropyridines as Correctors of the Cystic Fibrosis Transmembrane Conductance Regulator Channel Gating Defect Caused by Cystic Fibrosis Mutations. Mol. Pharmacol. 68(6) (2005) 1736-1746.

[12] N. Edraki, A.R. Mehdipour, M. Khoshneviszadeh, R. Miri, Dihydropyridines : evaluation of their current and future pharmacological applications. DDT 14 (2009) 1058-1066.

[13] P.J. Goodford, A Computational Procedure for Determining Energetically Favorable Binding Sites on Biological Important Macromolecules, J. Med. Chem. 28 (1985) 849-857.

[14] R.C. Wade, K.J. Clark, P.J. Goodford, Further Development of Hydrogen Bond Functions for Use in Determining Energetically Favorable Binding Sites on Molecules of Known Structure. 1. Ligand Probe Groups with the Ability To Form Two Hydrogen Bonds, J. Med. Chem. 36 (1993) 140-147.

[15] M. Pastor, G. Cruciani, I. Mclay, S. Pickett, S. Clementi, GRid-INdependent Descriptors (GRIND): A Novel Class of Alignment-Independent Three-Dimensional Molecular Descriptors, J. Med. Chem. 43 (2000) 3233-3243.

[16] M. Pastor, Development and Validation of AMANDA , a New Algorithm for Selecting Highly Relevant Regions in Molecular Interaction Fields, J. Chem. Inf. Mod. 48(9) (2008) 1813-1823.

[17] G. Cruciani, Molecular Interaction Fields - Applications in Drug Discovery and ADME Prediction, Wiley-CH, Zurich:, 2005.

[18] G. Ermondi, G. Caron, I.G. Pintos, M. Gerbaldo, M. Perez, D.I. Perez, Z. Gandara, A. Martinez, G. Gomez, Y. Fall, An application of two MIFs-based tools (Volsurf+ and Pentacle) to binary QSAR: the case of a palinurin-related data set of non-ATP competitive glycogen synthase kinase 3β (GSK-3β) inhibitors. Eur. J. Med. Chem. 46(3) (2011) 860-9.

[19] Organization for Economic Co-operation and Development. Guidance document on the validation of (quantitative) structure-activity relationship ((Q)SAR) models. OECD Series on Testing and Assessment 69 (OECD document ENV/JM/MONO) (2007) 55–65.

[20] G. Cruciani, P. Crivori, P. Carrupt, B. Testa, Molecular fields in quantitative structure – permeation relationships : the Volsurf+ approach, J. Mol. Struct.(THEOCHEM) 503 (2000)

17-30.

[21] T. Ogawa, A. Nakazato, K. Tsuchida, K. Hatayama, Synthesis and antihypertensive activities of new 1,4-dihydropyridine derivatives containing nitrooxyalkylester moieties and the 3- and 5-positions. Chem. Pharm. Bull. 41 (1993) 1049-1054.

[22] T. Ogawa, A. Nakazato, K. Tsuchida, K. Hatayama, Synthesis and antihypertensive activities of new 1,4-dihydropyridine derivatives containing a nitrooxy moiety at the 3-ester position. Chem. Pharm. Bull. 41 (1993) 108-116.

[23] D.G. Rhodes, J.G. Sarmiento, L.G. Herbette, Kinetics of Binding of Membrane-Active Drugs to Receptor Sites. Mol. Pharmacol. (1985), 27, 612-623.

[24] E. Carosati, R. Budriesi, P. Ioan, , M.P. Ugenti, M. Frosini, F. Fusi, G. Corda, B. Cosimelli, D. Spinelli, A. Chiarini, G. Cruciani, Discovery of Novel and Cardioselective Diltiazem- like Calcium Channel Blockers via Virtual Screening. J. Med. Chem. 51 (2008) 5552-5565.

[25] G. Ermondi, S. Visentin, G. Caron, GRIND-based 3D-QSAR and CoMFA to investigate topics dominated by hydrophobic interactions: the case of hERG K+ channel blockers. Eur. J. Med. Chem. 44(5) (2009), 1926-32.

[26] E. Raschi, L. Ceccarini, F.D. Ponti, M. Recanatini, hERG-related drug toxicity and models for predicting hERG liability and QT prolongation. Expert Opin. Drug Metab. Toxicol. 5(9) (2009), 1005-1022.

[27] G. Caron, G. Ermondi, Influence of Conformation on GRIND-Based Three-Dimensional Quantitative Structure-Activity Relationship (3D-QSAR), J. Med. Chem. 50 (2007) 5039-5042

[28] C. Medana, A. Di Stilo, S. Visentin, R. Fruttero, A. Gasco, D. Ghigo, A. Bosia, NO donor and biological properties of different benzofuroxans. Pharm. Res. (1999), 16, 956-960.

Caption to the figures

Figure 1. Chemical structures of the four DHPs of potential interest proposed by Pedemonte et al. in 2007 [6].

Figure 2. CFTR activators 3D-QSAR model: the linear relationship between the experimental and the calculated pK_d is shown together with the chemical structure of deviant compounds.

Figure 3. 3D-QSAR model for CFTR potentiators: filtered MIFs obtained with DRY (yellow), O (red). N1 (blue) and TIP (green) probes and the distance ranges corresponding to GRIND with VIPs value greater than 1.5. See text for model interpretation.

Figure 4. Calcium channel blocking 3D-QSAR model: filtered MIFs obtained with DRY (yellow), O (red). N1 (blue) and TIP (green) probes and the distance ranges corresponding to GRIND with VIPs value greater than 1.5. See text for model interpretation.

Figure 5. The histogram shows the original dataset solubility predicted by VolSurf+ expressed as -lg S 7.5 (the logarithm of solubility [mol/L] computed at pH 7.5, the lower the value, the less soluble the compound) together with **1** and **2** data. Compounds are ordered by decreasing potency as CFTR activators from the left to the right (the first bar on the left is due to the most potent compound, i.e. DHP194).

Figure 6. Molecules resulting from the *in silico* procedure.

Scheme 1. Synthetic procedure to obtain **2**.

Tables

Table 1. Statistical results for the best 3D-QSAR models (LVs = Latent Variables, r^2 = coefficient of determination, q^2 = model predictive ability by cross-validation, SDEP = standard deviation error of the prediction, precision = *tp/(tp+fp)* , recall = *tp/(tp+fn)*, accuracy = (*tp+tn)/(tp+tn+fp+fn)*, where *tp* is the number of true positives, *tn* is the number of true negatives, *fp* is the number of false positives and *fn* is the number of false negatives [18]).

CFTR activators		Calcium blockers	
Parameter	Value	Parameter	Value
LVs	4	LVs	3
r^2	0.85	Precision	0.95
q^2	0.50	Recall	1.00
SDEP	0.34	Accuracy	0.98

Table 2. ADME-Tox profile for hits compared with nifedipine. Values are reported with the threshold values discussed elsewhere [24].

Descriptor	**1**	**2**	Nifedipine	Lower threshold value	Upper threshold value
Log P_{oct}	3.53	2.86	2.45	1	5
LgS 7.5	-2.77	-2.86	-3.72	-4	Not set
Absorption	0.22	0.19	0.77	0.2	Not set
Lg BBB	1.39	1.40	-0.29		0
Metabolic stability	52.23	60.67	60.03	0.3	Not set
hERG [1]	5.50	6.20	4.11		6.0 (1μM)

[1] Calculated by the model reported by Ermondi et al. [25]

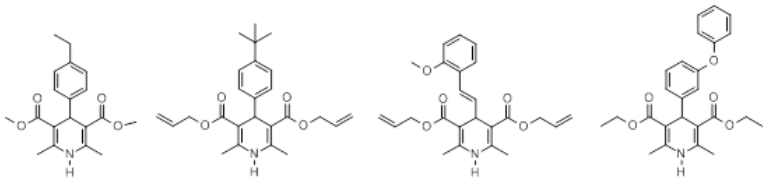

Figure 1

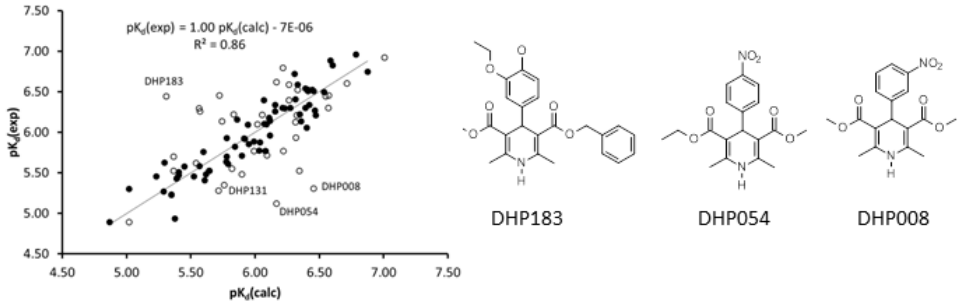
pKd(exp) = 1.00 pKd(calc) - 7E-06
R² = 0.86
DHP183
DHP131
DHP008
DHP054
pKd(exp)
pKd(calc)
7.50
7.00
6.50
6.00
5.50
5.00
4.50
4.50
5.00
5.50
6.00
6.50
7.00
7.50
DHP183
DHP054
DHP008

Figure 2

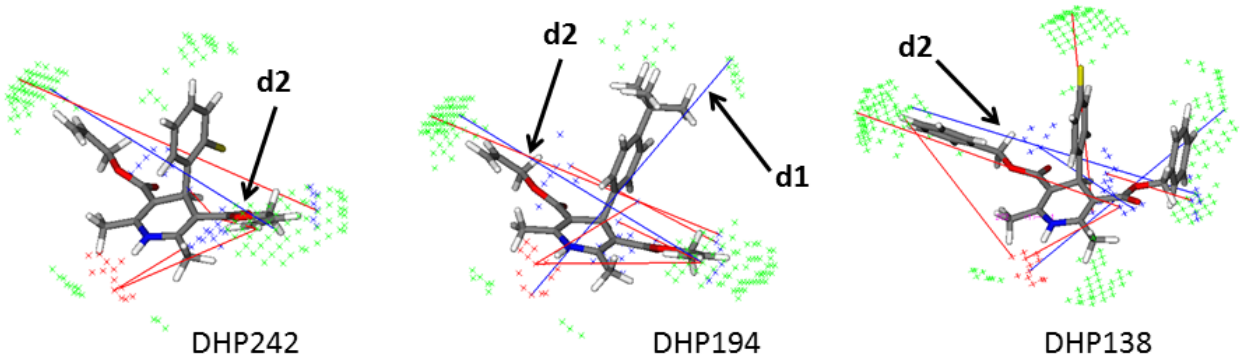

Figure 3

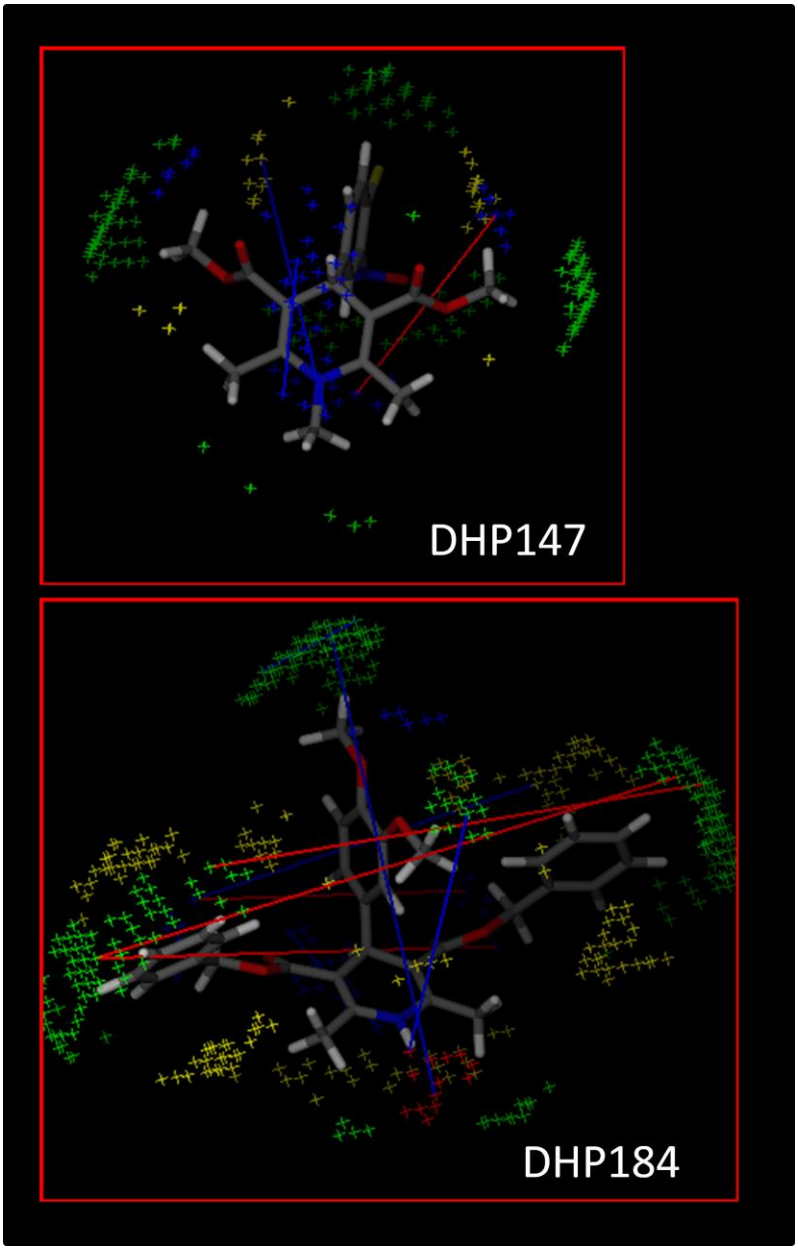

Figure 4

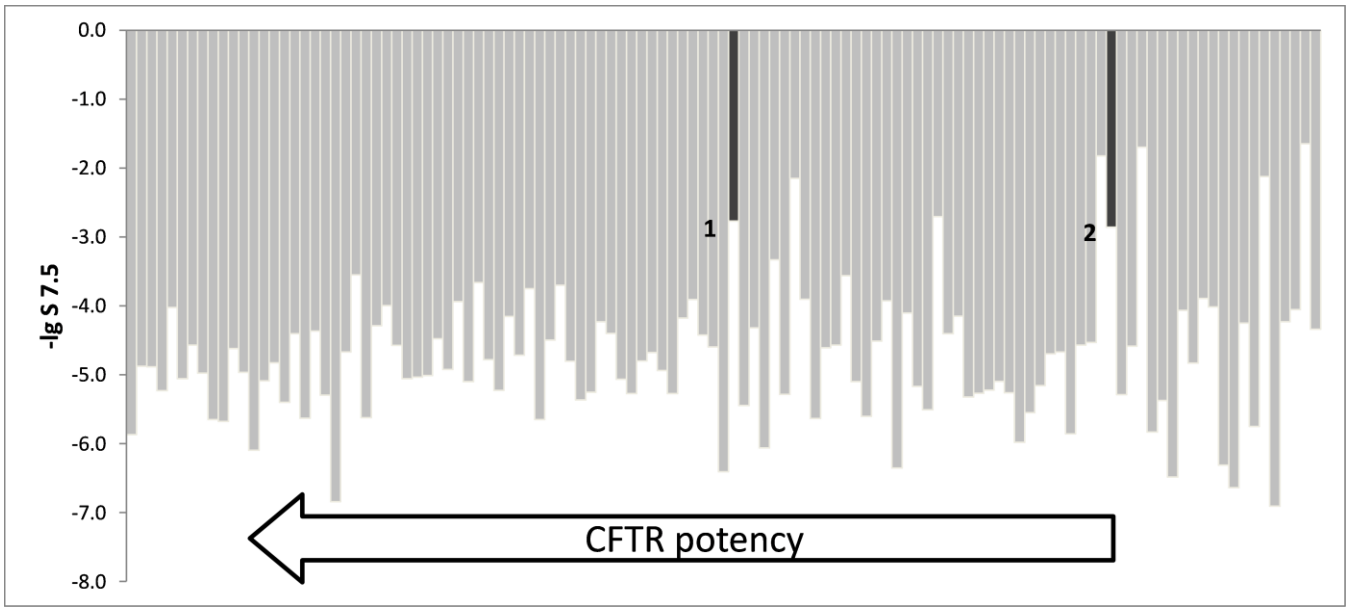

Figure 5

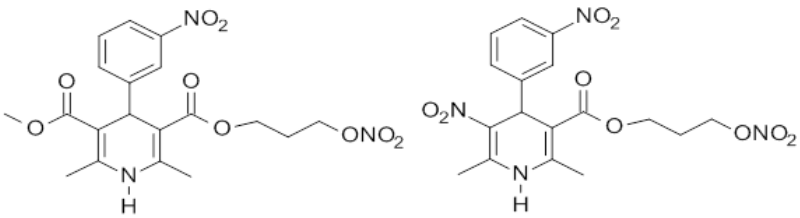

1 **2**

Figure 6

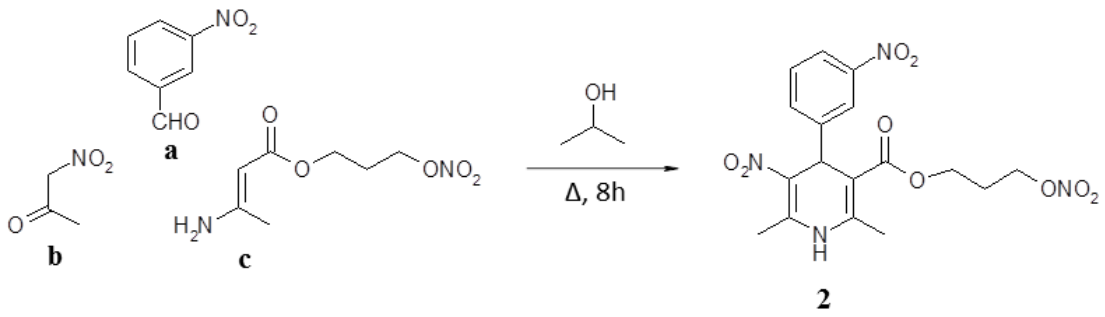

Scheme 1